Computer Assisted Methods in Engineering and Science, **22**: 329–346, 2015.

Macroscopic thermal properties of quasi-linear cellular medium on example of the liver tissue

Barbara Gambin, Eleonora Kruglenko,
Antoni Andrzej Gałka, Ryszard Wojnar
Institute of Fundamental Technological Research
Polish Academy of Sciences
Pawińskiego 5B, 02-106 Warszawa, Poland
e-mail: bgambin@ippt.gov.pl

There are two main topics of this research: (i) one topic considers overall properties of a nonlinear cellular composite, treated as a model of the liver tissue, and (ii) the other topic concerns the propagation of heat in the nonlinear medium described by the homogenised coefficient of thermal conductivity.

For (i) we give a method and find the effective thermal conductivity for the model of the liver tissue, and for the point (ii) we present numerical and analytical treatment of the problem, and indicate the principal difference of heat propagation in linear and nonlinear media. In linear media, as it is well known, the range of the heat field is infinite for all times $t > 0$, and in nonlinear media it is finite.

Pennes' equation, which should characterize the heat propagation in the living tissue, is in general a quasi-nonlinear partial differential equation, and consists of three terms, one of which describes Fourier's heat diffusion with conductivity being a function of temperature T. This term is just a point of our analysis.

We show that a nonlinear character of the medium (heat conductivity dependent on the temperature) changes in qualitative manner the nature of heat transfer. It is proved that for the heat source concentrated initially ($t = 0$) at the space point, the range of heated region (for $t > 0$) is finite. The proof is analytical, and illustrated by a numerical experiment.

Keywords: heat transport, asymptotic homogenisation, effective heat conductivity.

1. Introduction

1.1. Motivation of the research

The concept of ultrasound means sound waves with a frequency higher than 20 kHz, which is an approximate upper limit frequency of sounds audible by human ear. After the discovery of strong ultrasound generators (sonar systems) during the First World War, it was realized that the high-intensity ultrasound waves negatively influence biological organisms. For example, they can be used to heat and kill fish. These observations led to investigation of tissue heating by ultrasonic waves, and to study the effect of ultrasound on the state of health of the patient [1]. The contemporary state of the research is presented in [2] and [3].

On the other hand, this destructive ultrasonic action has been used in a lithotripsy procedure as a non-invasive treatment for the removal of kidney stones [4, 5].

The liver is both the largest internal organ and the largest gland in the human body. Its mass in an adult is about 1.5 kg. Lionel Smith Beale, FRS, (1828–1906), a surgeon, and promoter of microscopic studies in physiology and anatomy, in an expressive comparison wrote that the liver is like a great tree with its trunk, branches, and a myriad of leaves, which synthesize and purify the blood. Really, the liver has an autonomous circulatory system (the hepatic portal system comprising

the hepatic portal vein and its tributaries), and is composed of about one million primary lobules which are almost identical, like the leaves of the tree, cf. [6–11], also [12].

The liver constitutes only 2.5% of body weight, but it receives 25% of the cardiac output. As the result, the hepatic parenchymal cells are the most richly perfused of any cells in the human body. The total hepatic blood flow is about 120 ml/min per 100 g of liver, and one fifth to one third is supplied by the hepatic artery. About two thirds of the hepatic blood supply is portal venous blood [13].

The analysis of the heat diffusion in non-linear heterogeneous biological tissue is a subject of this paper. The research is partially based on studies described in [3]. Some of these results were reported at conferences [14, 15]. In addition, the homogenisation results of nonlinear media developed by the late Professor Józef Joachim Telega and his group [16, 17], are exploited below, and applied to non-stationary processes.

1.2. Structure of the paper

After a short review of the biological properties of the liver, we give mathematical description of its overall heat conductivity. Since the liver from mathematical point of view can be considered as a micro-periodic medium, the mathematical methods of homogenisation developed for micro-periodic media can be applied to determine some macroscopic properties of the tissue. Pennes' equation of heat propagation in biological tissue is a quasi-nonlinear partial differential equation with coefficients depending on temperature T. It consists of three terms, one describing Fourier's heat diffusion with the heat conductivity coefficient λ depending on T, second – the heat exchange due to blood perfusion, and third – the metabolic heat source rate.

Next, the homogenised heat conductivity coefficient is applied to a numerical simulation of the temperature diffusion produced by ultrasonic pulses and its simplified analytical description. Finally, we deal with a heat propagation in a nonlinear medium, and present a numerical simulation of the thermal effects of ultrasonic pulses. A method developed by Yakov Borisovich Zel'dovich and Aleksandr Solomonovich Kompaneets [18, 19], is used to interpret the simulation results.

2. Ultrasound in medicine

George Döring Ludwig (1922–1973), pioneer in application of ultrasounds in the medicine, found that the speed of ultrasound and acoustic impedance values of high water-content tissues are near to those of water. Namely, he found that the speed of sound in soft animal tissue is between 1490 and 1610 m/s, while the speed of sound in water is 1496 m/s (at 25°C). He also estimated the optimal scanning frequency of ultrasound transducer, as between 1 and 2.5 MHz [20].

The sound wave frequencies, and the corresponding velocities and wave-lengthes are given in the following table and are comparable with the dimensions of the hepatic lobule, which constitutes the basic *brick* of the liver structure, cf. Sec. 3.

Table 1. Ultrasound waves in the water.

Wave frequency [MHz]	Wave velocity [m/s]	Wave length [mm]
1	1 490	1.49
1	1 610	1.61
2.5	1 490	0.596
2.5	1 610	0.644

Advances in modern technology enable to satisfy requirements for the nondestructive characterization of material and biological properties in the μm range. An example of such a progress is

arising the acoustic microscopy, it is the microscopy that employs very high or ultra high frequency ultrasound [20, 21].

"Recent advances in the field have allowed acoustic microscope to be operated at wavelengths that correspond to the center of the optical band. Experimental results in the form of acoustic micrographs are presented and compared to their optical counterparts. It is apparent that the resolving power of these instruments is similar to that of the optical microscope" [22].

By using the reflection mode scanning acoustic microscope at nonlinear power levels, resolution beyond the linear diffraction limit can be achieved [23]. Profiting of relatively low attenuation of the ultrasonic waves at very high frequency, acoustic microscope can penetrate materials that are opaque to the visible light. Thus, acoustic microscopes reveal the ability to observe internal three-dimensional structures, unseen in the light [24].

In the acoustic microscopy the main problem is obtaining images of high resolution with minimum temperature increase, as this may be harmful for the tested biological specimens. Leszek Filipczyński with co-workers analyzed the propagation of heat in the lens of an acoustic microscope with a carrier frequency of 1 GHz, used for testing living cells at the frequency of 1 GHz [25–28].

3. Liver

The liver is composed of four lobes of unequal size and shape, with rich micro-structure. The liver is an important vital organ with a wide range of functions including protein synthesis and storage, transformation of carbohydrates, synthesis of cholesterol, bile salts and phospholipids, detoxification, and production of biochemicals necessary for digestion [8, 29].

3.1. Lobules

Each liver lobe is made up of hepatic lobules. In the mentioned Beale's comparison, these lobules correspond to the leaves of a tree. The shape of the hepatic lobule is approximately hexagonal, and divided into concentric parts, with the central vein in the middle, see Fig. 1. The lobule is about $2 \times 1 \times 2$ mm in size [30]. Thus, its dimensions are comparable with ultrasonic wave-lengthes from Table 1.

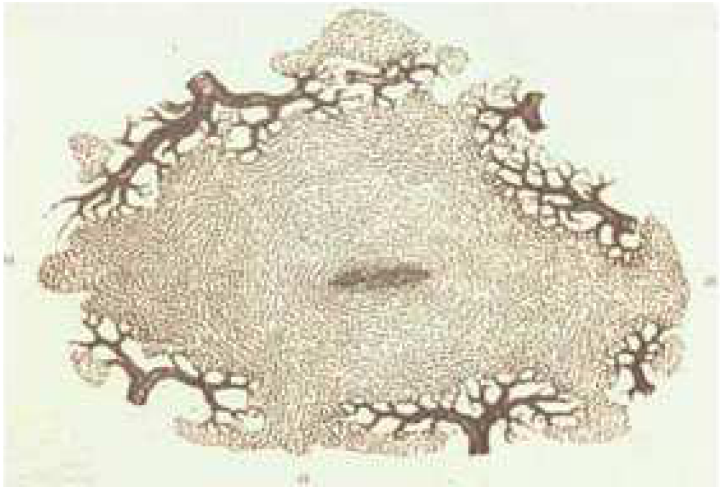

Fig. 1. Beale's drawing of a single lobule (real size about $2 \times 1 \times 2$ mm). The blood enters the lobule at its periphery, and a tiny network of capillaries, or sinusoids, runs through it to the central hepatic vein. There are also portal triads on the border of the lobule.

Each lobule is containing at least 1000 sinusoids 0.5–1.0 mm in length, and 700 nm in breadth. One can estimate there are over 1 billion sinusoids in the liver.

Another component of the hepatic lobule is a portal triad. It consists of the following five elements: proper hepatic artery, hepatic portal vein, common bile duct, lymphatic vessels, and a branch of the vagus nerve. The name *portal triad* is a traditional and now confusable. It was given before lymphatic vessels and the branch of the nerve were discovered in the structure.

The hepatic lobules also consist of plates of hepatocytes radiating from a central vein. A hepatocyte is a cell of the main parenchymal tissue of the liver. Hepatocytes make up 70–85% of the liver's mass. The typical hepatocyte is similar to a cube with sides of 20–30 μm.

Sinusoidal capillaries are a special type of open-pore capillary also known as a discontinuous capillary, that have larger openings (30–40 μm in diameter) in the endothelium [31].

From a metabolic meaning, the functional unit of the liver is the hepatic acinus (liver acinus, terminal acinus). The hepatic acinus is a diamond-shaped mass of liver parenchyma surrounding a portal tract, and is smaller than a portal lobule. Its longer diagonal extends between central hepatic veins of two adjacent lobuli, and the shorter diagonal extends between the two nearest portal triads, cf. [32].

3.2. Cellular structure of the liver and its heat conductivity

The liver can be considered as an unidirectional composite of the lobules, the plane normal to the central vein direction can be considered as the isotropic plane, at sufficiently long wavelengths (low frequencies) of acoustic excitation. The central vein of each lobule is along the axis that is normal to the plane of isotropy.

Each layer of lobules has approximately the same properties in-plane but different properties through-the-thickness. The plane of each layer is the plane of isotropy and the vertical axis is the axis of symmetry. Thus it is a material with a transversal isotropy. A transversely isotropic material is one with physical properties which are symmetric about an axis that is normal to a plane of isotropy.

The heat conductivity of a transversely isotropic material is described by the matrix [33],

$$\boldsymbol{\lambda} = \begin{vmatrix} \lambda_{11} & 0 & 0 \\ 0 & \lambda_{11} & 0 \\ 0 & 0 & \lambda_{33} \end{vmatrix}$$

with two different elements, λ_{11} and λ_{33}.

4. Thermal properties and pennes' equation

The heat in a living body is transferred by three different mechanisms: conduction, convection (natural or forced) and radiation. Average thermal conductivity of the liver in $(\mathrm{W}/(\mathrm{m}\cdot\mathrm{K})$ is 0.52 with standard deviation 0.03. The same numbers are found for the blood [34]. The tissue temperature $T = T(\mathbf{r}, t)$ depends on the spacial position $\mathbf{r} = (x_k)$, $k = 1, 2, 3$ and the time t. Pennes' equation deals with description of the tissue temperature T and reads [35, 36],

$$c\,\rho\frac{\partial T}{\partial t} = \frac{\partial}{\partial x_k}\left(\lambda(T)\frac{\partial T}{\partial x_k}\right) + w_b\,c_b\,\rho_b(T_a - T) + q. \tag{1}$$

Here, ρ and c are the mass density $[\mathrm{kg/m^3}]$ and specific heat $[\mathrm{J}/(\mathrm{kg}\cdot\mathrm{K})]$ of the tissue, respectively, $w_b = w_b(\mathbf{r}, t)$ is the blood perfusion rate $[\mathrm{m^3}$ blood/(s kg tissue)], c_b – blood specific heat, ρ_b – blood density, T_a is the temperature of the arterial supply blood. The heat generation term q encompasses the thermal effects of metabolism and, if necessary, other volumetric heat loads, as microwave irradiation or the heat generated by ultrasound waves.

4.1. Nonlinearity of thermal properties

There is considerable variation in the thermal properties from tissue to tissue, from species to species, and even within tissues from the same donor. The thermal properties of water taken from [37] were fit to a linear equation over the range 0° to 45°, it is $\lambda = 0.5652 + 0.001575\,T$. The thermal conductivity of tissue is lower than that of water, while the temperature dependence approximates that of water, cf. also [38, 39].

Therefore, for the biological materials we observe the linear dependence of the heat conductivity on temperature

$$\lambda = a + bT \tag{2}$$

and the experimental data are gathered in the Table 2.

Table 2. Linear dependence of the heat conductivity on temperature in the water and the collagen, cf. Eq. (2).

Substance	a	b	Temperature range
Water	0.5652	0.001575	0–45°C
Sheep collagen	0.5280	0.001729	25–50°C

The thermal conductivity λ is given in $\mathrm{W}\cdot\mathrm{m}^{-1}\cdot\mathrm{K}^{-1}$ units.

4.2. One-dimensional time-independent problem

Let the section $[x_0, x_0+\ell]$ of x axis consist of two sub-sections (segments) $[x_0, x_0+a]$ and $[x_0+a, x_0+\ell]$. Let the heat conductivity be $\lambda_{\mathrm{a}}(1+\alpha T)$ in $[x_0, x_0+a]$ and $\lambda_{\mathrm{b}}(1+\beta T)$ in $[x_0+a, x_0+\ell]$.

Consider time independent heat flow described by the equation

$$\begin{aligned} &\frac{\mathrm{d}}{\mathrm{d}x}\left\{\lambda_{\mathrm{a}}(1+\alpha T)\frac{\mathrm{d}T}{\mathrm{d}x}\right\} = 0 \quad \text{for} \quad x_0 < x < x_0 + a, \\ &\frac{\mathrm{d}}{\mathrm{d}x}\left\{\lambda_{\mathrm{b}}(1+\beta T)\frac{\mathrm{d}T}{\mathrm{d}x}\right\} = 0 \quad \text{for} \quad x_0 + a < x < x_0 + \ell, \end{aligned} \tag{3}$$

together with the boundary conditions $T(x_0) = T_0$ and $T(\ell) = T_\ell$. The conservation of the heat energy density stream imposes that the integration constants appearing after the first integration in both cases are the same and equal C. After second integration we get

$$\lambda_{\mathrm{a}}\left\{\left(T_{\mathrm{a}} + \frac{1}{2}\alpha T_{\mathrm{a}}^2\right) - \left(T_0 + \frac{1}{2}\alpha T_0^2\right)\right\} = Ca \quad \text{and} \quad \lambda_{\mathrm{b}}\left\{\left(T_\ell + \frac{1}{2}\alpha T_\ell^2\right) - \left(T_{\mathrm{a}} + \frac{1}{2}\alpha T_{\mathrm{a}}^2\right)\right\} = C(\ell - a). \tag{4}$$

The quantity T_{a} denotes the unknown temperature at $x = x_0 + a$. By solving the last set

$$T_{\mathrm{a}} = \frac{b\lambda_{\mathrm{a}} + a\lambda_{\mathrm{b}}}{b\lambda_{\mathrm{a}}\alpha + a\lambda_{\mathrm{b}}\beta} \times \left\{-1 + \sqrt{1 + 2\frac{b\lambda_{\mathrm{a}}\alpha + a\lambda_{\mathrm{b}}\beta}{(b\lambda_{\mathrm{a}} + a\lambda_{\mathrm{b}})^2}\left(b\lambda_{\mathrm{a}}\left(T_0 + \frac{1}{2}\alpha T_0^2\right) + a\lambda_{\mathrm{b}}\left(T_\ell + \frac{1}{2}\beta T_\ell^2\right)\right)}\right\}. \tag{5}$$

For small α and β we expand the square term in series and obtain

$$T_{\mathrm{a}} = \frac{1}{b\lambda_{\mathrm{a}} + a\lambda_{\mathrm{b}}}\left(b\lambda_{\mathrm{a}}\left(T_0 + \frac{1}{2}\alpha T_0^2\right) + a\lambda_{\mathrm{b}}\left(T_\ell + \frac{1}{2}\beta T_\ell^2\right)\right). \tag{6}$$

In the linear case, for $\alpha = 0$ and $\beta = 0$ we have

$$T_{\mathrm{a}} = \frac{1}{b\lambda_{\mathrm{a}} + a\lambda_{\mathrm{b}}}\left(b\lambda_{\mathrm{a}}T_0 + a\lambda_{\mathrm{b}}T_\ell\right) \tag{7}$$

and observe that for $\alpha > 0$ and $\beta > 0$ the nonlinear expression for the temperature T_{a} is always greater than the linear one.

5. Effective thermal conductivity of the liver

5.1. Nonlinear heat transport

Effective medium approximations are descriptions of a medium (composite material) based on the properties and the relative fractions of its components. To these approximations belongs Clausius-Mossotti's formula (CMF) for the effective conductivity of the medium consisting of the matrix substance of conductivity λ_M, in which are disseminated small spherical inclusions of conductivity λ_I. If the ratio of the volume of all small spheres to that of whole is f, then

$$\lambda^{\text{eff}} = \frac{\lambda_I + 2\lambda_M + 2(\lambda_I - \lambda_M)f}{\lambda_I + 2\lambda_M - (\lambda_I - \lambda_M)f}\lambda_M. \tag{8}$$

Vladimir Mityushev gave the definition of the effective thermal conductivity for the case when the conductivity coefficient is a function of the temperature T, and found a generalization of CMF for a family of strongly non-linear and weakly inhomogeneous composites [40].

A. Gałka, J.J. Telega and S. Tokarzewski using asymptotic methods derived the formula for the effective heat conductivity in this general case [16]. In one-dimensional case their formula reads

$$\lambda^{\text{eff}} = A(\xi) + B(\xi) + \frac{C(\xi)}{T - D(\xi)}, \tag{9}$$

where $\xi = a/\ell$, and A, B, C, D are given function of ξ. Their effective conductivity λ^{eff} is no more linear in the temperature.

5.2. Homogenisation

We study a quasi-linear heat equation for periodically micro-heterogeneous medium, and perform asymptotic homogenisation of the problem [41, 42].

Let $\Omega \subset I\!R^3$ be a bounded regular domain and $\Gamma = \partial\Omega$ its boundary. We introduce a parameter

$$\varepsilon = \frac{l}{L}, \tag{10}$$

where l and L are typical length scales of micro-inhomegeneities and the region Ω, respectively.

The small parameter ε characterizes the micro-structure of the material. Hence, the coefficients and the fields of the problem are functions of the ε, what indicates superscript ε.

Performing homogenisation, or passing with ε to zero one obtains the homogenised (known also as the effective) coefficients. Such procedure is possible, since in the local problem the macroscopic temperature $T^{(0)}$ plays the role of a parameter only.

We are going to study the non-stationary heat equation

$$\begin{aligned} &\rho^\varepsilon c^\varepsilon \frac{\partial T^\varepsilon}{\partial t} = \frac{\partial}{\partial x_i}\left(\lambda_{ij}^\varepsilon \frac{\partial T^\varepsilon}{\partial x_i}\right) + r^\varepsilon \qquad \text{in} \quad \Omega, \\ &T^\varepsilon = 0 \qquad\qquad\qquad\qquad\qquad\quad \text{on} \quad \partial\Omega. \end{aligned} \tag{11}$$

Above ρ^ε and c^ε denote the density of the material and its specific heat, respectively. The both quantities have a microstructure denoted by the superscript ε. Moreover, we admit that the specific heat can depend on the temperature T

$$c^\varepsilon = c\left(\frac{x}{\varepsilon}, T\right) \qquad \text{for} \quad x \in \Omega. \tag{12}$$

Similarly, the heat conductivity

$$\lambda_{ij}^{\varepsilon} = \lambda_{ij}\left(\frac{x}{\varepsilon}, T\right) \qquad \text{for} \quad x \in \Omega \tag{13}$$

and $r^{\varepsilon} = r(x, x/\varepsilon, t)$ denotes a heat source, positive or negative, dependent on the microstructure also.

The heat equation (11) includes, as a special case Pennes' equation (1) provided that

$$r^{\varepsilon} = w_b^{\varepsilon}\, c_b^{\varepsilon}(T - T_a) + q^{\varepsilon}. \tag{14}$$

The time dependent Eq. (11) is also a generalization of a stationary quasi-linear heat equation, treated by Gałka, Telega and Tokarzewski [16, 17].

By Y we denote the so-called basic cell, for instance

$$Y = (0, Y_1) \times (0, Y_2) \times (0, Y3).$$

We assume the symmetricity of the heat conduction tensor

$$\lambda_{ij} = \lambda_{ji} \tag{15}$$

and assume also that it is positive definite

$$\lambda_{ij}\xi_i\,\xi_j \geq \alpha_0|\xi|^2 \tag{16}$$

for all $\xi \in I\!R^3$.

According to the method of two-scale asymptotic expansions we write

$$T^{\varepsilon} = T^{(0)}(x, y) + \varepsilon T^{(1)}(x, y) + \varepsilon^2\, T^{(2)}(x, y) + \cdots, \tag{17}$$

where

$$y \equiv \frac{x}{\varepsilon} \tag{18}$$

and the functions $T^{(0)}(x, y)$, $T^{(1)}(x, y)$, $T^{(2)}(x, y)$, and so on, are Y-periodic. Hence, we write

$$\lambda_{ij}(y, T^{(0)}(x, y) + \varepsilon\, T^{(1)}(x, y) + \varepsilon^2 T^{(2)}(x, y) + \cdots) = \lambda_{ij}(y, T^{(0)}) + \varepsilon\, T^{(1)}\frac{\partial \lambda_{ij}(y, T^{(0)})}{\partial T^{(0)}}$$
$$+ \varepsilon^2\left(T^{(2)}\frac{\partial \lambda_{ij}(y, T^{(0)})}{\partial T^{(0)}} + \frac{1}{2}(T^{(1)}(x, y))^2\frac{\partial^2 \lambda_{ij}(y, T^{(0)})}{\partial (T^{(0)})^2}\right) + \cdots. \tag{19}$$

For sake of the brevity, we omit the dependence on the time t in the written arguments of the functions introduced in the expansion (17).

It is tacitly assumed that all derivatives appearing in the asymptotic homogenisation make sense. We recall that for a function $f(x, y)$, where $y = x/\varepsilon$ the operator $\partial/\partial x_i$ should be replaced by

$$\frac{\partial}{\partial x_i} + \frac{1}{\varepsilon}\frac{\partial}{\partial y_i}.$$

According to the method of asymptotic homogenisation we compare the terms associated with the same power of ε.

5.3. Results of the homogenisation

We successively obtain:
at ε^{-2}

$$\frac{\partial}{\partial y_j}\left(\lambda_{ij}\left(y,T^{(0)}(x,y)\right)\frac{\partial T^{(0)}(x,y)}{\partial y_i}\right)=0 \tag{20}$$

what is satisfied provided that $T^{(0)}$ does not depend on the local variable y, it is

$$T^{(0)}=T^{(0)}(x). \tag{21}$$

This statement holds true under the assumption that the coefficients $\lambda_{ij}\left(y,T^{(0)}(x,y)\right)$ are positive definite and Y-periodic. Again, for sake of the brevity we omit the argument t in (20) and (21);
at ε^{-1}

$$\frac{\partial}{\partial y_j}\left\{\lambda_{ij}\left(y,T^{(0)}(x)\right)\left(\frac{\partial T^{(0)}(x)}{\partial x_i}+\frac{\partial T^{(1)}(x,y)}{\partial y_i}\right)\right\}=0 \tag{22}$$

at ε^{0}, after integration over Y,

$$\rho c\frac{\partial T^{(0)}}{\partial t}=\frac{\partial}{\partial x_j}\left\{\frac{1}{|Y|}\int\limits_Y\lambda_{ij}\left(y,T^{(0)}(x)\right)\left(\frac{\partial T^{(0)}(x)}{\partial x_i}+\frac{\partial T^{(1)}(x,y)}{\partial y_i}\right)+r(x,y,t)\right\}\mathrm{d}y, \tag{23}$$

where

$$T^{(1)}(x,y)=\frac{\partial T^{(0)}(x)}{\partial x_i}\chi_k\left(y,T^{(0)}\right). \tag{24}$$

The local functions $\chi_k(y,T^{(0)})$, $k=1,2,3$ are solutions to the local problem

$$\frac{\partial}{\partial y_j}\left\{\lambda_{ij}\left(y,T^{(0)}(x)\right)\left(\frac{\partial\chi_k\left(y,T^{(0)}(x)\right)}{\partial y_i}+\delta_{ik}\right)\right\}=0. \tag{25}$$

Finally, substitution of $T^{(1)}$ from (24) into Eq. (23) gives

$$\overline{\rho\,c}\frac{\partial T^{(0)}(x,t)}{\partial x_j}=\frac{\partial}{\partial x_j}\left(\lambda_{ij}^{\mathrm{eff}}\left(T^{(0)}(x,t)\right)\frac{\partial T^{(0)}(x,t)}{\partial x_i}\right)+\overline{r}(x,t). \tag{26}$$

The quantity $T^{(0)}=T^{(0)}(x,t)$ is interpreted as the macroscopic temperature $T=T(x,t)$. Moreover,

$$\overline{\rho\,c}=\frac{1}{|Y|}\int\limits_Y\rho\,c\,\mathrm{d}y\qquad\text{and}\qquad\overline{r}(x,t)=\frac{1}{|Y|}\int\limits_Y r(x,y,t)\,\mathrm{d}y. \tag{27}$$

The effective tensor of heat conductivity in Eq. (26) reads

$$\lambda_{ij}^{\mathrm{eff}}\left(T^{(0)}(x,t)\right)=\frac{1}{\|Y\|}\int\limits_Y\left\{\lambda_{ij}\left(y,T^{(0)}\right)+\lambda_{kj}\left(y,T^{(0)}\right)\frac{\partial\chi_i}{\partial y_k}\right\}\mathrm{d}y \tag{28}$$

with the local function χ_i being a solution of Eq. (25).

6. Homogenised coefficients

Consider a system built of elementary long tubes. Each tube constitutes a simplified model of the hepatic lobule, cf. Sec. 3. Its middle part, the central vein is represented as a channel, filled in reality with the blood and enclosed in the collagen sheath. In our calculation we take the water instead of the blood, because the water is well defined physical substance, and as it was explained, it has almost the same heat conductivity as the blood.

In homogenisation procedure the cross-section of the tube (the hepatic lobule) is treated as a basic cell Y. It is approximated by a square with the unit side, cf. Fig. 2. The cross-section of the inner channel is denoted by Y_1, and the cross-section of the exterior collagen sheath by Y_2. In general, the cross-section Y_1 is a rectangle, with sides ξ and η, and its points satisfy inequalities

$$Y_1 = \left(-\frac{\xi}{2}, \frac{\xi}{2}\right) \times \left(-\frac{\eta}{2}, \frac{\eta}{2}\right) \qquad \text{while} \qquad Y_2 = Y \backslash Y_1. \tag{29}$$

We use the thermal properties of both components given in Subsec. 4.1.

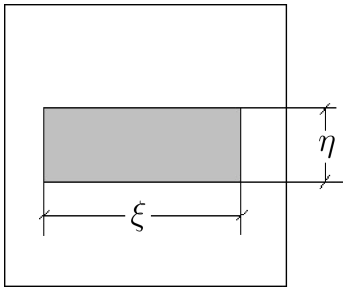

Fig. 2. Basic cell Y. The square is 1×1, while the inner rectangle $\xi \times \eta$.

6.1. Ritz' method

To find approximation of the local functions χ_i we apply Ritz' method, cf. [16, 43, 44]. We make an assumption

$$\chi_i = \sum_a \chi_{ia}(T)\phi_a(y), \tag{30}$$

where $\phi_a(y)$, $a = 1, 2, \cdot, n$ are prescribed Y-periodic functions and $\chi_{ia}(T)$ are unknown constants.

The weak (variational) formulation of Eq. (25) reads: find $\chi_k(\cdot, T^{(0)}) \in H_{\text{per}}(Y)$ such that

$$\int_Y \left\{ \lambda_{ij}\left(y, T^{(0)}(x)\right)\left(\frac{\partial \chi_k\left(y, T^{(0)}(x)\right)}{\partial y_i} + \delta_{ik}\right)\right\} \frac{\partial v(y)}{\partial y_i} \mathrm{d}y = 0 \tag{31}$$

for each $v \in H_{\text{per}}(Y)$.

The local problem (31) should be satisfied for test functions of the form

$$v = v_a\, \phi_a(y). \tag{32}$$

To determine the unknown constants one has to solve the following algebraic equation

$$\chi_{ia}\, A_{ab} = B_{ib}, \tag{33}$$

where

$$A_{ab}(T) = \int_Y \lambda_{ij}(y,T)\frac{\partial\phi_a(y)}{\partial y_i}\frac{\partial\phi_b(y)}{\partial y_j}\,\mathrm{d}y \quad \text{and} \quad B_{ib}(T) = -\int_Y \lambda_{ij}(y,T)\frac{\partial\phi_b(y)}{\partial y_j}\,\mathrm{d}y. \tag{34}$$

For a given macroscopic temperature T the solution of Eq. (33) is

$$\chi_{ia} = (\mathbf{A}^{-1})_{ab}\,B_{ib}, \tag{35}$$

where $\mathbf{A}^{-1}$ is the inverse matrix of $\mathbf{A}$. Finally, we obtain

$$\lambda_{ij}(T)^{\mathrm{eff}} = \langle\lambda_{ij}(y,T)\rangle + (\mathbf{A}^{-1}(T))_{ab}\,B_{ib}(T)\,B_{ja}(T). \tag{36}$$

In the two-dimensional case $y = (y_1, y_2)$, $\partial\phi_a(y)/\partial y_3 = 0$. Then, after (34) we get

$$A_{ab}(T) = \lambda^{(2)}(T)\int_Y \frac{\partial\phi_a(y)}{\partial y_i}\frac{\partial\phi_b(y)}{\partial y_i}\,\mathrm{d}y_1\,\mathrm{d}y_2 + [\lambda^{(2)}(T) - \lambda^{(1)}(T)]\int_{Y_1}\frac{\partial\phi_a(y)}{\partial y_i}\frac{\partial\phi_b(y)}{\partial y_i}\,\mathrm{d}y_1\,\mathrm{d}y_2$$

and (37)

$$B_{ib}(T) = [\lambda^{(2)}(T) - \lambda^{(1)}(T)]\int_{Y_1}\frac{\partial\phi_b(y)}{\partial y_i}\,\mathrm{d}y_1\,\mathrm{d}y_2.$$

The base functions are taken in the form

$$\phi_1(y_1,y_2) = \begin{cases} \xi y_1 + \dfrac{\xi}{2} & \text{if} \quad y_1 \in \left(-\dfrac{1}{2}, -\dfrac{\xi}{2}\right), \\ -(1-\xi)y_1 & \text{if} \quad y_1 \in \left(-\dfrac{\xi}{2}, \dfrac{\xi}{2}\right), \\ \xi y_1 - \dfrac{\xi}{2} & \text{if} \quad y_1 \in \left(\dfrac{\xi}{2}, \dfrac{1}{2}\right), \end{cases} \tag{38}$$

$$\phi_2(y_1,y_2) = \begin{cases} \eta y_2 + \dfrac{\eta}{2} & \text{if} \quad y_2 \in \left(-\dfrac{1}{2}, -\dfrac{\eta}{2}\right), \\ -(1-\eta)\,y_2 & \text{if} \quad y_2 \in \left(-\dfrac{\eta}{2}, \dfrac{\eta}{2}\right), \\ \eta y_2 - \dfrac{\eta}{2} & \text{if} \quad y_2 \in \left(\dfrac{\eta}{2}, \dfrac{1}{2}\right). \end{cases} \tag{39}$$

Substituting the functions (38) and (39) into (37), and subsequently into (36), we find the approximate dependence of the effective conductivity $\lambda_{ij}^{\mathrm{eff}}(T)$ on the temperature T.

6.2. Calculated coefficients

Our basic cell of periodicity is composed of two parts, internal inclusion, short "in", and external, short "ex", see Fig. 2, and in our case, both parts are made of isotropic materials. The heat conductivities taken from Table 2, for the water and the collagen, respectively, can be written in the matrix form as

$$\lambda_{ij}^{(\mathrm{in})} = w\begin{bmatrix} 1 & 0 \\ 0 & 1 \end{bmatrix} \qquad \text{and} \qquad \lambda_{ij}^{(\mathrm{ex})} = k\begin{bmatrix} 1 & 0 \\ 0 & 1 \end{bmatrix}, \tag{40}$$

where w and k are given scalar functions of the temperature T. Then the components of the effective heat conductivity tensor read

$$\lambda_{11}^{\text{eff}}(T) = \xi w\eta + (1-\xi\eta)\,k - \frac{\eta^2\xi(1-\xi)\,(k-w)^2}{\eta(1-\xi)(k-w)-k}, \tag{41}$$

$$\lambda_{22}^{\text{eff}}(T) = \xi w\eta + (1-\xi\eta)\,k - \frac{\xi^2\eta(1-\eta)\,(k-w)^2}{\xi(1-\eta)(k-w)-k}. \tag{42}$$

We observe that the linear term of the homogenised conductivity is simple arithmetic mean of conductivities of the components.

6.3. Homogenisation results

In our calculations we take as the inner material – the water, and as the external one – the collagen. Hence, cf. Subsec. 4.1,

$$w = 0.5652 + 0.001575\,T \qquad \text{and} \qquad k = 0.5280 + 0.001729\,T. \tag{43}$$

In calculated examples we consider two different cases, one isotropic, and the second – anisotropic, see Fig. 3.

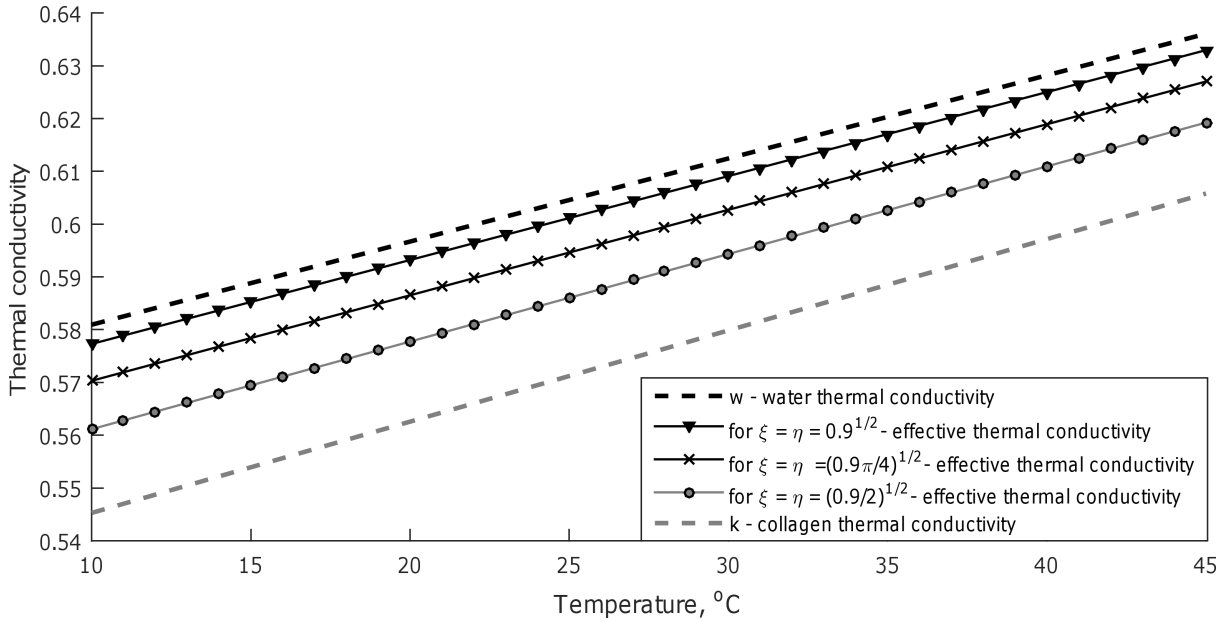

Fig. 3. The effective conductivity tensor components in isotropic composite ($\lambda_{11}^{\text{eff}} = \lambda_{22}^{\text{eff}}$) as the function of the temperature T for three different square inclusions.

First, an *isotropic* micro-heterogeneous medium is studied, with the basic cell characterized by $\xi = \eta = \sqrt{0.9}$, what corresponds to 90% amount of the water in the tissue. In Fig. 3 the temperature dependence of the effective conductivity components of the homogenised medium is shown. We have $\lambda_{11}^{\text{eff}}(T) = \lambda_{22}^{\text{eff}}(T)$ in this case. The lower fraction of the water manifests in moving away the effective lines from the line of water conductivity.

In the second case, the basic cell is characterized by $\xi = 0.71$ and $\eta = 0.99$, what corresponds to 70% of the water amount in the tissue, and should result in the anisotropy of the homogenised

medium. The difference of the effective conductivity components $(\lambda_{11}^{\text{eff}}(T) - \lambda_{22}^{\text{eff}}(T))$ in function of the temperature T is presented in Fig. 4. Both lines are different, but still very near each other; the difference is less than 4×10^{-4}. We observe that the difference does not depend on the temperature.

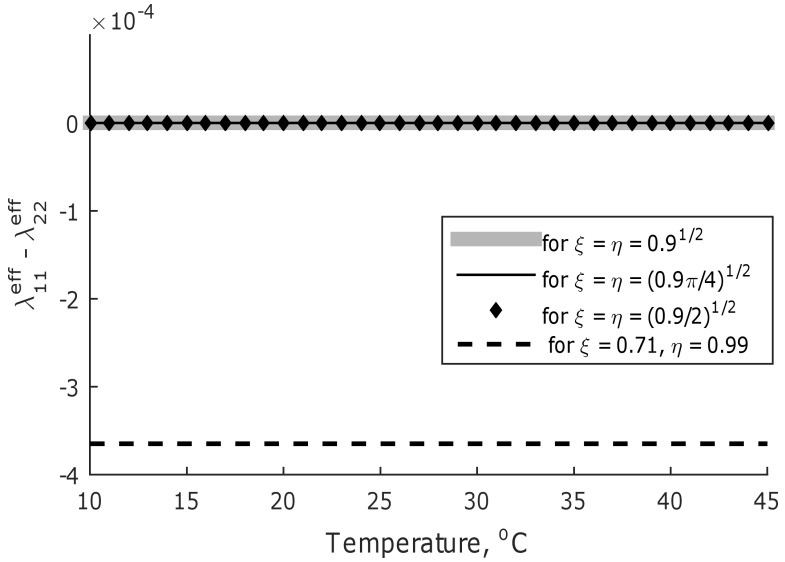

Fig. 4. The difference of the effective conductivity tensor components $(\lambda_{11}^{\text{eff}} - \lambda_{22}^{\text{eff}})$ for both, isotropic and anisotropic composites does not depend on the temperature T. The basic cell of the isotropic composite is built of the square water inclusion in the collagen matrix; the water inclusion for the anisotropic case has the shape of rectangle 0.71×0.99.

6.4. Estimation of the method error

We began our calculations for the material built of square cells with a circular opening inside. This circular opening we call the *initial circle*. Next, we replaced a circular opening by a square one. Such a procedure entails an methodical error. To estimate it we carried out 3 similar tasks with different square inclusions: (i) the side of square is equal to diameter $2R = \sqrt{0.9}$ of the replaced circle (circumscribed square), (ii) square of the surface equal to the initial circle, and (iii) inscribed square. The results are shown in Fig. 3. The discrepancies are smaller than 2%.

7. Application to numerical FEM calculations

To determine the temperature field inside the liver tissue, a numerical model based on the finite element method (FEM) was implemented in the Abaqus 6.12 software (DS SIMULIA Corp.). This numerical model simulates an experiment of heating the liver tissue sample *in vitro* by ultrasound circular focusing transducer, described in [45] and [2]. The axially-symmetric problem is considered, in which an ultrasound wave is propagating in the positive z axis direction. The temperature fields are induced by ultrasound circular focusing transducer, with the focus placed inside the liver sample *in vitro* immersed in the water bath. The dimensions of the longitudinal cross-section of the calculation area are 40×15 mm. The dimensions of the longitudinal cross-section of the focus area are 20×2.25 mm, see Fig. 5.

The transducer is immersed in water and the source acoustic power is 0.7 W, and 50% of the acoustical energy is transformed into heat [46]. The time of exposure was 2 seconds. Thus the heat energy supplied to the tissue is 0.7 J. The coefficients in the heat transfer equation solved numerically are assumed as follows. The temperature dependent heat conductivities are given by Eq. (2) and Table 2, the densities and the specific heats of water and tissue are 1000 and 1060 kg/m^3, and 4200 and 3600 J/kg K, respectively.

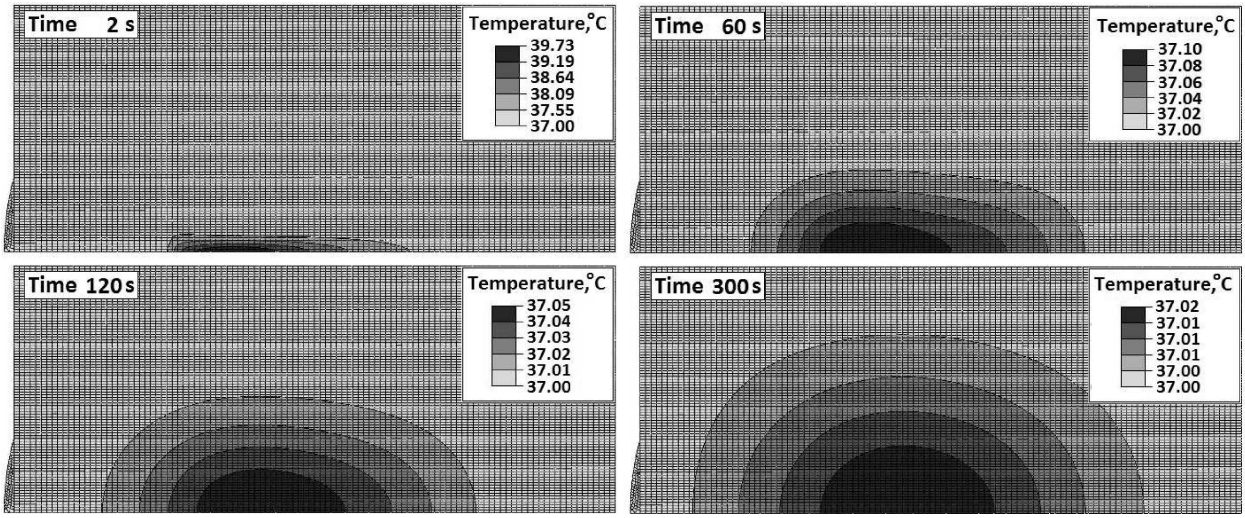

Fig. 5. The propagation of the heat pulse in the liver. Profiting the symmetry, the half of the image is shown only. The z-axis – the direction of the ultrasonic wave. Notice that the range of the temperature scale changes from image to image due to lowering of the temperature.

7.1. Propagation of heat pulse in nonlinear medium

Since the deflection from rectilinearity in the dependence of the effective heat conductivity λ^{eff} is very small, cf. Fig. 3, we assume that after homogenisation the function $\lambda^{\text{eff}} = \lambda^{\text{eff}}(T)$ it is still linear. Hence, we consider a propagation of a thermal pulse (produced by a focused ultrasound beam) in the medium with the conductivity λ linear in T

$$\lambda = \lambda_0(1 + bT), \tag{44}$$

with λ_0 and b being positive constants

$$\lambda = \lambda_0(1 + bT) \geq 0. \tag{45}$$

At the initial instant, $t = 0$, an amount of heat Q is concentrated at the point $x = 0$, while $T = T_0$ every where else

$$T^0(x, t = 0) \equiv T^0(x, 0) = Q\delta(x). \tag{46}$$

The heat equation has the form

$$\frac{\partial T}{\partial t} = a\frac{\partial}{\partial x}\left\{(1 + bT)\,\frac{\partial T}{\partial x}\right\}, \tag{47}$$

where

$$a = \frac{\lambda_0}{c_p} = \text{constant} \tag{48}$$

and c_p is the specific heat at constant pressure.

We introduce a rescaled temperature G by the substitution

$$G = 1 + bT \qquad \text{or} \qquad T = \frac{G - 1}{b} \tag{49}$$

gives

$$\frac{\partial G}{\partial t} = a\frac{\partial}{\partial x}\left(G\frac{\partial G}{\partial x}\right). \tag{50}$$

Now, we can apply the method developed by Zel'dovich and Kompaneets [18, 19], also [48], and look for a solution in the form

$$G = \left(\frac{Q^2}{at}\right)^{1/3} f(\xi), \tag{51}$$

where

$$\xi = \frac{x}{(Qat)^{1/3}} \tag{52}$$

is a dimensionless variable. We get subsequently

$$\frac{\partial G}{\partial t} = -\frac{1}{3}\left(\frac{Q^2}{a}\right)^{1/3}\frac{1}{t^{4/3}}\left(f + \xi\frac{\mathrm{d}f}{\mathrm{d}\xi}\right) \quad \text{and} \quad \frac{\partial G}{\partial x} = \frac{Q^{1/3}}{(a\,t)^{2/3}}\frac{\mathrm{d}f}{\mathrm{d}\xi}. \tag{53}$$

Moreover

$$\frac{\partial^2 G}{\partial x^2} = \frac{1}{a\,t}\frac{\mathrm{d}^2 f}{\mathrm{d}\xi^2}. \tag{54}$$

Therefore

$$\frac{\partial}{\partial x}\left(G\frac{\partial G}{\partial x}\right) = \left(\frac{\partial G}{\partial x}\right)^2 + G\frac{\partial^2 G}{\partial x^2} = \frac{Q^{2/3}}{(a\,t)^{4/3}}\frac{\mathrm{d}}{\mathrm{d}\xi}\left(f\frac{\mathrm{d}f}{\mathrm{d}\xi}\right). \tag{55}$$

With the substitution (51), the equation (50) reads

$$\frac{\mathrm{d}}{\mathrm{d}\xi}\left(\xi\,f + 3\,f\frac{\mathrm{d}f}{\mathrm{d}\xi}\right) = 0. \tag{56}$$

This ordinary differential equation has a solution

$$f = \frac{1}{6}\left(\xi_0^2 - \xi^2\right) + C \tag{57}$$

which satisfies the conditions of the problem. We put

$$C = \left(\frac{Q^2}{at}\right)^{-1/3} \tag{58}$$

and returning to the expression (51), we get

$$G = \left(\frac{Q^2}{at}\right)^{1/3}\frac{1}{6}\left(\xi_0^2 - \xi^2\right). \tag{59}$$

This formula gives the distribution of the rescaled temperature G in the interval between the points $x = \pm x_0$, corresponding at every instant to the equations $\xi = \pm\xi_0$

$$x_0 = (Qat)^{1/3}\xi_0. \tag{60}$$

The temperature field expands with time as $x_0 \propto t^{1/3}$, and outside the interval $[-\xi_0, \xi_0]$ the temperature vanishes, $T = 0$.

The constant ξ_0 is determined by the condition that the total amount of the heat energy be constant. The respective law of energy conservation reads

$$\int_{-\infty}^{\infty} T(x,t)\,\mathrm{d}x = \int_{-\infty}^{\infty} T^0(x,0)\,\mathrm{d}x = Q. \tag{61}$$

The expression (60) together with (59) can be compared with the numerical experiment results, in which the locality and finite range of the heat impulse are observed, cf. Fig. 5.

8. Results and conclusions

Accounting for the nonlinearity in Pennes' equation results in qualitative (and obviously quantitative) change of heat propagation, in comparison with a linear medium.

First, the dimension of the heated region is always finite, while in the classical description it always infinite. This result finds its confirmation in FEM calculations for the heat transport in the homogeneous liver tissue described by the temperature dependent effective heat conductivity.

Second, the appropriability of the used model of heat transport was affirmed by experimental measurements of the temperature field in a rat liver, cf. [2]. The heating was realized by focusing an ultrasound beam, while the temperature of the liver during its ultrasound heating was measured by thermocouples. The linear equation, it is the heat equation with constant conductivity did not describe the time dependence of the temperature increase in the region of the most strong heating, even quantitatively. Quite the opposite, the FEM calculations, in which the temperature dependence of the heat conductivity was accounted for, permitted for much better fitting of the experimental curve [47]. The power of heat sources used in our FEM calculations was determined independently from a model of focusing an ultrasound wave in absorbing medium [49].

Applying the homogenisation method to find nonlinear properties of heat transport in two-component cellular materials permits to discuss the influence of two main components of the soft tissue, it is of the collagen and the water, for the effective thermal conductivity. It was shown that almost linear dependence of the effective conductivity on temperature is retained, and the values of the effective conductivity are moving closer to the water values, see Fig. 3.

To obtain the effective thermal conductivity of the composite, a simplified periodic geometry of structure of type inclusion in matrix was introduced. The elementary (basic) cell was composed of the square collagen matrix with a rectangular inclusion (of sides ξ and η), filled with the water. For such a configuration we could realize maximally possible anisotropy. As is shown in Fig. 4, for $\xi = 0.71$ and $\eta = 0.99$, the difference $(\lambda_{11}^{\mathrm{eff}} - \lambda_{22}^{\mathrm{eff}})(T)$, being an indicator of the anisotropy is less than 4×10^{-4} what gives a relative discrepance of the order $10^{-3}\%$. This means that even in this case the anisotropy of heat conductivity is small, what justifies our simplified calculation, in which we applied a square basic cell (instead of the hexagonal one).

The second simplification, which we have made, pertains to modelling of the cross-section of a blood vessel, which is a circle or ellipse, and which in our calculations was replaced by a square. This permitted to elucidate the procedure, the main aim of which was to prove that the heat propagation in tissues with a structure of two-phase composites of the type collagen-water, and of overall isotropic properties in the interval 36–43°C can be described with high accuracy by the effective heat conductivity.

In Fig. 3 we make a comparison of the effective conductivity for 3 different, albeit similar basic cells, in which the circular opening filled with the water is replaced by (a) the square circumscribed over the circle, (b) the square of the surface equal to the surface of the circle, and (c) the square inscribed into the circle. We observe that the conductivities found for these 3 cases agree within relative discrepancies less than 10^{-5}.

In the algebraic formulae (41) and (42) the following parameters take place: the heat conductivities of the components (as functions of the temperature, for example, for the collagen and the water), and the geometrical proportions (ξ and η) of the water inclusion. These formulae permit to evaluate the thermal conductivity of the composite, in function of the fraction of components.

The hepatic lobule, the elementary brick of the liver tissue was considered as the basic cell in the homogenisation process. It was shown that for this tissue, in this what concerns the heat conductivity it is sufficient to replace the hexagonale structure by the square lattice.

The following results are obtained:

- mathematical formulation of the problem of nonlinear heat conductivity of the liver,
- introduction of a mathematical model of the liver, being a cellular composite prepared of the collagen skeleton fulfilled with the water,
- calculation of the homogenised heat conductivity coefficients for the above composite,
- the numerical experiment on heat propagation in the liver characterized by calculated homogenised coefficients,
- the analysis of the results of the numerical experiment by Zel'dovich and Kompaneets' approach.

We have evaluated the dependence of the effective conductivity on the temperature T for the homogeneous (in large scale) cutting of the liver. The cutting was treated as a two-dimensional periodic composite, built of lobules, imitated by the collagen capillaries filled with the water.

The linear dependance of the conductivity coefficient holds for the liver tissue, as a result of small differences (small contrast) of the heat coefficients of the tissue components.

Acknowledgement

This work was partially supported by the National Science Center (grant no. 2011/03/B/ ST7/ 03347).

References

[1] Walter G. Cady. *Piezoelectricity*. McGraw-Hill, New York and London, 1946.
[2] B. Gambin, E. Kruglenko, T. Kujawska, M. Michajłow. Modeling of tissues *in vivo* heating induced by exposure to therapeutic ultrasound. *Acta Physica Polonica* A, **119**(6A): 950–956, 2011.
[3] E. Kruglenko, B. Gambin, L. Cieślik. Soft tissue-mimicking materials with various numbers od scatterers and their acoustical characteristics. *Hydroacoustics*, **16**: 121–128, 2013.
[4] L. Filipczyński, J. Etienne. Capacitance hydrophones for pressure determination in lithotripsy. *Ultrasound. Med. Biol.*, **16**(2): 157–165, 1990.
[5] A. Srisubat, S. Potisat, B. Lojanapiwat, V. Setthawong, M. Laopaiboon. Extracorporeal shock wave lithotripsy (ESWL) versus percutaneous nephrolithotomy (PCNL) or retrograde intrarenal surgery (RIRS) for kidney stones. *The Cochrane Library*, **11** CD007044 (24 November 2014).
[6] L.S. Beale. *On some points in the anatomy of the liver of man and vertebrate animals, with directions for injecting the hepatic ducts, and making preparations*. Illustrated with upwards of sixty photographs of the authors drawings, London, John Churchill, London, 1856.
[7] L.S. Beale. *How to Work with the Microscope*. 4th edition, Harrison, London, 1868.
[8] L.S. Beale. *The liver*, Illustrated with eighty-six figures, copied from nature, many of which are coloured, J.&A. Churchill, London 1889; *The Journal of Physiology*, Vol. 10, Iss. 5, 1 JUL 1889.
[9] A. Bochenek, M. Reicher. *Anatomia człowieka. Tom II. Trzewa*, wydanie VIII (V), Wydawnictwo Lekarskie PZWL, Warszawa, 1998.
[10] V. Kumar, A.K. Abbas, J.C. Aster. *Robbins and Cotran pathologic basis of disease*. Ninth edition, Chapter 18. *Liver and gallbladder*, Elsevier Saunders, Philadelphia, PA, 2015.
[11] *Liver*, from Wikipedia, the free encyclopedia, https://en.wikipedia.org/wili/Liver.
[12] *The Hepatic Ultrastructure*, http://www.otago.ac.nz/christchurch/research/liversieve/otago0120971.html.

[13] *Hepatic Circulation: Physiology and Pathophysiology*, http://www.ncbi.nlm.nih.gov/books/NBK53069/.
[14] R. Wojnar, B. Gambin. Thermal properties of biomaterials on the example of the liver. The 3rd Polish Congress of Mechanics, Gdańsk, September 8–11, 2015.
[15] B. Gambin, E. Kruglenko, R. Wojnar. Macroscopic thermal properties of quasi-linear cellular medium on example of the liver tissue, Numerical Heat Transfer 2015 – Eurotherm Seminar No 109, Institute of Thermal Technology, Silesian University of Technology, Gliwice, Institute of Heat Engineering, Warsaw University of Technology, 27–30 September 2015, Warszawa.
[16] A. Gałka, J.J. Telega, S. Tokarzewski. Nonlinear transport equation and macroscopic properties of microheterogeneous media. *Arch. Mech.*, **49**(2): 293–310, 1997.
[17] J.J. Telega, M. Stańczyk. Modelling of soft tissues behaviour. [In:] *Modelling in biomechanics*, J.J. Telega [Ed.], Institute of Fundamental Technological Research Polish Academy of Sciences, pp. 191–453, Warsaw 2005.
[18] Ya B. Zeldovich, A.S. Kompaneets. The theory of heat propagation in the case where conductivity depends on temperature. [In:] *Collection of papers celebrating the seventieth birthday of Academician A.F. Ioffe*, P.I. Lukirskii [Ed.], Izdat. Akad. Nauk SSSR, Moskva, pp. 61–71, 1950, (in Russian).
[19] L.D. Landau, E.M. Lifshitz. *Fluid Mechanics*, Volume 6 of Course of Theoretical Physics, transl. from the Russian by J.B. Sykes and W.H. Reid, Second edition, Pergamon Press, Oxford – New York – Beijing – Frankfurt – Sao Paulo – Sydney – Tokyo – Toronto, 1987.
[20] J. Woo. *A Short History of the Development of Ultrasound in Obstetrics and Gynecology*. E-source Discovery Network, University of Oxford, retrieved March 12, 2012.
[21] L.W. Kessler. *Acoustic Microscopy*. Metals Handbook, Vol. 17 – Nondestructive Evaluation and Quality Control, ASM International, pp. 465–482, 1989.
[22] V. Jipson, C.F. Quate. Acoustic microscopy at optical wavelengths, *Appl. Phys. Lett.*, **32**(12): 789–791, 1978.
[23] D. Rugar. Resolution beyond the diffraction limit in the acoustic microscope: A nonlinear effect. *J. Appl. Phys.*, **56**(5): 1338–1346, 1984.
[24] K. Dynowski, J. Litniewski. Three-dimentional imaging in ultrasonic microscopy. *Archives of Acoustics*, **32**(4S): 71–75, 2007.
[25] T. Kujawska, J. Wójcik, L. Filipczyński. Possible temperature effects computed for acoustic microscopy used for living cells. *Ultrasound in Medicine and Biology*, **30**(1): 93–101, 2004.
[26] H. Carslow, J. Jaeger. *Conduction of Heat in Solids*, Oxford: Clarendon Press, Russian translation, Nauka, Moskva, 1964.
[27] H. Tautz. *Warmeleitung und Temperaturausgleich*, Akademie Verlag, p. 37, Berlin, 1971.
[28] L. Filipczyński. Estimation of heat distribution in the acoustic lens of an ultrasonic microscope with the carrier frequency of 1 GHz. *Archives of Acoustics*, **29**(3): 427–433, 2004.
[29] R.S. Cotran, V. Kumar, N. Fausto, F. Nelso, S.L. Robbins, A.K. Abbas. *Pathologic Basis of Disease*, 7th edition, Elsevier Saunders, St. Louis, MO 2005.
[30] Liver Sieve Research Group Liver Structure, http://www.otago.ac.nz/christchurch/research/liversieve/otago0120971.html.
[31] H.F. Teutsch, D. Schuerfeld, E. Groezinger. Three-dimensional reconstruction of parenchymal units in the liver of the rat. *Hepatology*, **29**(2): 494–505, 1999.
[32] B.R. Bacon, J.G. O'Grady, A.M. Di Bisceglie, J.R. Lake. *Comprehensive Clinical Hepatology*. Elsevier Health Sciences, Philadelphia, 2006.
[33] L.D. Landau, E.M. Lifshitz. *Theory of Elasticity*, Volume 7 of Course of Theoretical Physics, transl. by J.B. Sykes and W.H. Reid, 3rd edition, Pergamon Press, Oxford – New York – Toronto – Sydney – Paris – Braunschweig, 1975.
[34] http://www.itis.ethz.ch/itis-for-health/tissue-properties/database/thermal-conductivity/.
[35] H.H. Pennes. Analysis of tissue and arterial blood temperatures in the resting human forearm. *J. Appl. Physiol.*, **1**(2): 93–122, 1948.
[36] Z. Ostrowski, P. Buliński, W. Adamczyk, A.J. Nowak. Modelling and validation of transient heat transfer processes in human skin undergoing local coolong. *Przegląd Elektrotechniczny*, **91**(5): 76–79, 2015.
[37] Y.S. Touloukian, P.E. Liley, S.C. Saxena. in *Thermophysical Properties of Matter*, The TPRC Data Series (IFI/Plenum, New York, 1970), Vol. 3, pp. 120, 209; Vol. 10, pp. 290, 589.
[38] J.W. Valvano, J.R. Cochran, K.R. Diller. Thermal conductivity and diffusivity of biomaterials measured with self-heated thermistors. *International Journal of Thermophysics* (*Intern. J. Thermophysics*), **6**(3): 301–311, 1985.
[39] A. Bhattacharya, R.L. Mahajan. Temperature dependence of thermal conductivity of biological tissues. *Physiological Measurement*, **24**(3): 769–783, 2003.
[40] V. Mityushev. First order approximation of effective thermal conductivity for a non-linear composite. *J. Tech. Phys.*, **36**(4): 429–432, 1995.
[41] E. Sanchez-Palencia. *Non-Homogeneous Media and Vibration Theory*. Springer Verlag, Berlin, Heidelberg, New York, 1980.
[42] N.S. Bakhvalov, G.P. Panasenko. *Homogenisation: Averaging Processes in Periodic Media*: *Mathematical Problems in the Mechanics of Composite Materials*. Nauka, Moscow, 1984 (in Russian); English transl. Kluwer, Dordrecht – Boston – London, 1989.

[43] A. Gałka, J.J. Telega, R. Wojnar. Thermodiffusion in heterogeneous elastic solids and homogenization. *Arch. Mech.*, **46**: 267–314, 1994.
[44] A. Gałka, J.J. Telega, R. Wojnar. Some computational aspects of homogenization of thermopiezoelectric composites. *Comput. Assist. Mech. Eng. Sci.*, **3**(2): 133–154, 1996.
[45] T. Kujawska, J. Wójcik, A. Nowicki. Numerical modeling of ultrasound-induced temperature fields in multilayer nonlinear attenuating media. *Hydroacoustics*, **12**: 91–98, 2009.
[46] J. Wójcik. Conservation of energy and absorption in acoustic fields for linear and nonlinear propagation. *The Journal of the Acoustical Society of America*, **104**(5): 2654–2663, 1998.
[47] E. Kruglenko. The influence of the physical parameters of tissue on the temperature distribution during ultrasound interaction [in Polish: Wpływ zmienności właściwości fizycznych tkanki na rozkład temperatury w tkance przy terapeutycznym oddziaływaniu ultradźwięków]. *Biomedical Engineering* [in Polish: *Inżynieria Biomedyczna*], **18**(4): 250–254, 2012.
[48] R. Wojnar. Subdiffusion with external time modulation. *Acta Physica Polonica*, **114**(3): 607–611, 2008.
[49] T. Kujawska, W. Secomski, E. Kruglenko, K. Krawczyk, A. Nowicki. Determination of tissue thermal conductivity by measuring and modeling temperature rise induced in tissue by pulsed focused ultrasound. *PLOS ONE*, **9**(4): e94929–1–8, 2014.